Cell

Article

# Metabolic trade-offs constrain the cell size ratio in a nitrogen-fixing symbiosis

## Graphical abstract

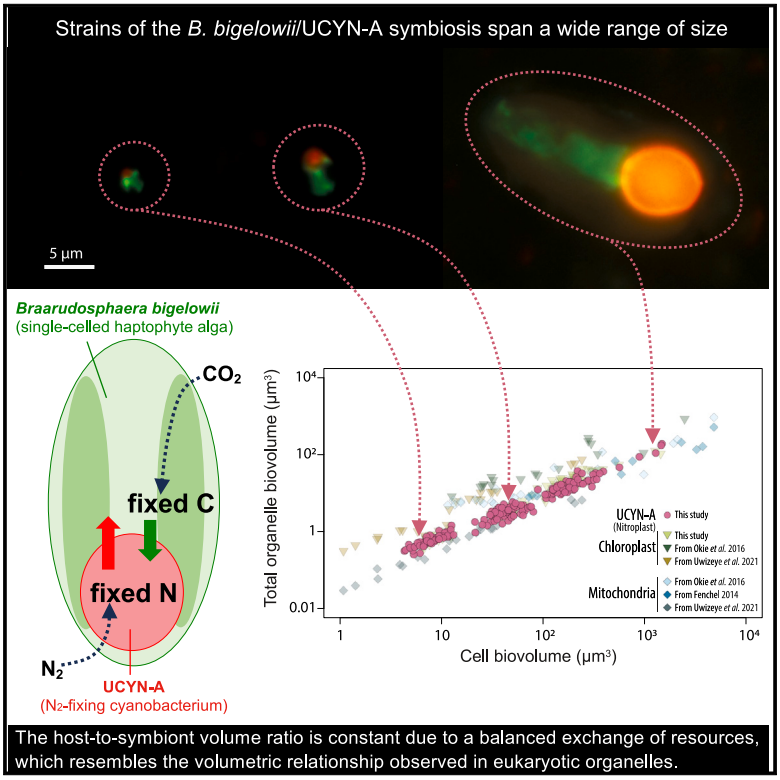


## Highlights

- Strong volume covariation in the *B. bigelowii*/UCYN-A nitrogen-fixing symbiosis
- The constant volumetric relationship reflects symbiotic resource economy constraints
- Coordination of harvesting and exchange of resources maximizes symbiotic growth rate
- UCYN-A is functioning like a hypothetical $N_2$-fixing organelle (or nitroplast)

## Authors

Francisco M. Cornejo-Castillo, Keisuke Inomura, Jonathan P. Zehr, Michael J. Follows

## Correspondence

fmcornejo@icm.csic.es (F.M.C.-C.), inomura@uri.edu (K.I.)

## In brief

The robust volumetric relationship between partners of a marine planktonic nitrogen-fixing symbiosis reflects predictable, balanced, and quantitative interdependencies among $CO_2$ fixation, respiration, and $N_2$ fixation that maximize synchronized growth rate.

Cornejo-Castillo et al., 2024, Cell *187*, 1762–1768
March 28, 2024 
https://doi.org/10.1016/j.cell.2024.02.016

CellPress

CellPress
OPEN ACCESS

Cell

Article

# Metabolic trade-offs constrain the cell size ratio in a nitrogen-fixing symbiosis

Francisco M. Cornejo-Castillo,[1,2,6,7,*] Keisuke Inomura,[3,6,*] Jonathan P. Zehr,[2,5] and Michael J. Follows[4,5]
[1]Department of Marine Biology and Oceanography, Institut de Ciències del Mar, ICM-CSIC, Barcelona 08003, Spain
[2]Department of Ocean Sciences, University of California, Santa Cruz, CA 95064, USA
[3]Graduate School of Oceanography, University of Rhode Island, Narragansett, RI 02882, USA
[4]Department of Earth, Atmospheric, and Planetary Sciences, Massachusetts Institute of Technology, Cambridge, MA 02139, USA
[5]Senior author
[6]These authors contributed equally
[7]Lead contact
*Correspondence: fmcornejo@icm.csic.es (F.M.C.-C.), inomura@uri.edu (K.I.)
https://doi.org/10.1016/j.cell.2024.02.016

## SUMMARY

Biological dinitrogen ($N_2$) fixation is a key metabolic process exclusively performed by prokaryotes, some of which are symbiotic with eukaryotes. Species of the marine haptophyte algae *Braarudosphaera bigelowii* harbor the $N_2$-fixing endosymbiotic cyanobacteria UCYN-A, which might be evolving organelle-like characteristics. We found that the size ratio between UCYN-A and their hosts is strikingly conserved across sublineages/species, which is consistent with the size relationships of organelles in this symbiosis and other species. Metabolic modeling showed that this size relationship maximizes the coordinated growth rate based on trade-offs between resource acquisition and exchange. Our findings show that the size relationships of $N_2$-fixing endosymbionts and organelles in unicellular eukaryotes are constrained by predictable metabolic underpinnings and that UCYN-A is, in many regards, functioning like a hypothetical $N_2$-fixing organelle (or nitroplast).

## INTRODUCTION

Nitrogen (N) is essential for life on Earth. Despite the large reservoir of atmospheric dinitrogen ($N_2$) gas, primary producers depend on "fixed" forms of N such as nitrate or ammonium, which can be largely limiting in ecosystems such as the oligotrophic open ocean. Only some Bacteria and Archaea ($N_2$-fixers or diazotrophs) are able to reduce $N_2$ to ammonium ($N_2$ fixation), which makes them essential for the maintenance of primary productivity in diverse ecosystems.[1–3] However, $N_2$ fixation is also widespread in eukaryotes through symbioses with diazotrophs, including some cyanobacteria, which are common in aquatic and terrestrial environments.[1,4]

One symbiotic $N_2$-fixing bacterium is the cyanobacterium *Candidatus* Atelocyanobacterium thalassa (hereafter, UCYN-A), which might be evolving organelle-like characteristics. Natural populations of closely related sublineages of UCYN-A live as endosymbionts with a closely related group of species of the haptophyte microalga *Braarudosphaera bigelowii*,[2,5,6] all uncultivated except for one set of coastal strains[6] (Figure 1A). UCYN-A are phylogenetically related to cyanobacteria but have a greatly reduced genome and are metabolically streamlined, having lost the enzymes needed for carbon (C) fixation, the tricarboxylic acid cycle, and photosystem II that is necessary for oxygenic photosynthesis in cyanobacteria.[7] On the other hand, UCYN-A have retained the entire set of $N_2$ fixation genes and provide fixed N to their hosts, which in turn provide UCYN-A with C fixed photosynthetically by its chloroplasts.[2] *B. bigelowii* and its closely related species are eukaryotic calcifying algae with two chloroplasts per cell[8] that have both calcareous and naked flagellate life stages, and one UCYN-A spheroid body is physically located within the host cell between the two chloroplasts in the *B. bigelowii* calcified form[5] and at the posterior side of the naked flagellate form in culture[6] (Figure 1A). UCYN-A is surrounded by a single host membrane, engulfed in what is thought to be the host's food vacuole.[5,6,9] In the open ocean and coastal environments, closely related species of *B. bigelowii* display a large variation in cell length (10-fold, from 2 to 3 μm up to 20–30 μm) and harbor genetically distinct but closely related UCYN-A sublineages (UCYN-A1, -A2, and -A3 sublineages) (Figure 1C), which also range 10-fold in effective cell radius and up to ca. 1,000-fold in cell volume.[5,10–12] There is significant empirical evidence that the per-cell photosynthesis rate of diverse, marine free-living phytoplankton taxa, including haptophytes, exhibits power-law relationships with cell volume.[13–17] However, it is unclear whether this allometric relationship holds in phytoplankton taxa harboring endosymbionts that fully depend on the C fixation of their hosts, which is the case with UCYN-A.[18] On the other hand, it is also unknown whether $N_2$ fixation in UCYN-A affects the cell size of their haptophyte

 

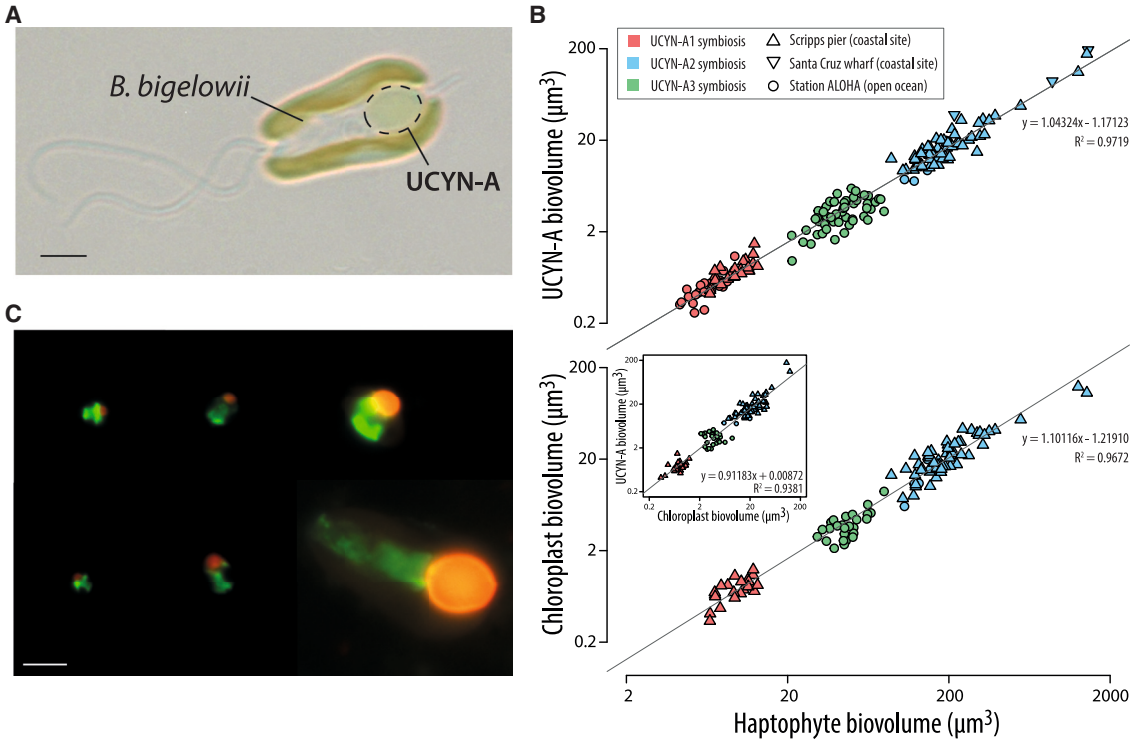


**Figure 1. Linear volumetric scaling in the *B. bigelowii*/UCYN-A symbiosis**

(A) Light microscopy image of the haptophyte *B. bigelowii* in symbiosis with UCYN-A (scale bar, 2 µm; image courtesy of Wing Kwan Esther Mak and Kyoko Hagino).

(B) Upper panel: UCYN-A volume (sublineages UCYN-A1, -A2, and -A3; see inset) as a function of associated haptophyte cell volume; lower panel: chloroplast volume as a function of associated haptophyte cell volume; inset in lower panel: UCYN-A volume vs. chloroplast volume of associated host cells.

(C) Composite of catalized reporter deposition fluorescence *in situ* hybridization (CARD-FISH) images showing the range of sizes of the different UCYN-A sublineages (left images: UCYN-A1 sublineage; middle images: UCYN-3 sublineage; right images: UCYN-A2 sublineage) and their symbiotic haptophyte partners. Images were taken under blue (green-labeled haptophytes with Alexa 488 stain) and green (red-labeled UCYN-A with Alexa 594 stain) excitation wavelengths (STAR Methods) (scale bar, 5 µm).

See also Figure S1.

symbiotic partners in an analogous way to photosynthesis in marine phytoplankton. The large cell size variation that is observed across the multiple closely related UCYN-A lineages and *B. bigelowii* species in symbiotic partnerships provides a unique opportunity to explore the metabolic underpinnings of these host/symbiont cell size relationships and, ultimately, might explain the role of size in the evolution of symbiotic interactions.

## RESULTS AND DISCUSSION

### Strong size relationship between UCYN-A and its host

We measured the size of three different UCYN-A sublineages (UCYN-A1, UCYN-A2, and UCYN-A3), their symbiotic haptophyte partner cells, and their corresponding chloroplasts in many tens of symbiotic pairs (N = 167), collected from environmental samples representing a wide range of oceanic nutrient conditions, and estimated their corresponding biovolumes (Figure 1B; Table S1) (STAR Methods). We found a remarkably consistent linear relationship between the total volume of the haptophyte cells (i.e., the volume of *B. bigelowii* + UCYN-A) and the volume occupied by UCYN-A within its host that holds true within and across different sublineages ($\log_{10}(V_{UCYN\text{-}A}) = 1.0\ \log_{10}(V_{hapto}) - 1.2$, $R^2 = 0.97$, $p < 10^{-16}$, linear regression analysis; Figure 1B), which corresponds with an average ratio of the effective haptophyte cell and UCYN-A radii ($R_H/R_D$) of 2.33 (±0.20) (Figure 2C). Within one of these sublineages (UCYN-A1), a previous study also reported a linear relationship ($R^2 = 0.93$) between the cell diameter of UCYN-A and their haptophyte partners based on a small number of measurements (N = 7).[19] A recent study found a similar positive and significant relationship between the cell length of the marine diatom *Rhizosolenia* and the trichome length of the symbiotic filamentous $N_2$-fixing cyanobacteria species *R. intracellularis*,[20] a length-based relationship that also holds true in the *B. bigelowii*/UCYN-A symbiosis (Figure S1).

### Metabolic constraints of the size relationship

The strong covariation of haptophyte and UCYN-A body size in the *B. bigelowii*/UCYN-A symbiosis, and similar covariations in other $N_2$-fixing symbioses,[20] imply a robust and common underlying mechanism. We hypothesized that these relationships reflect the maximization of a synchronized growth rate

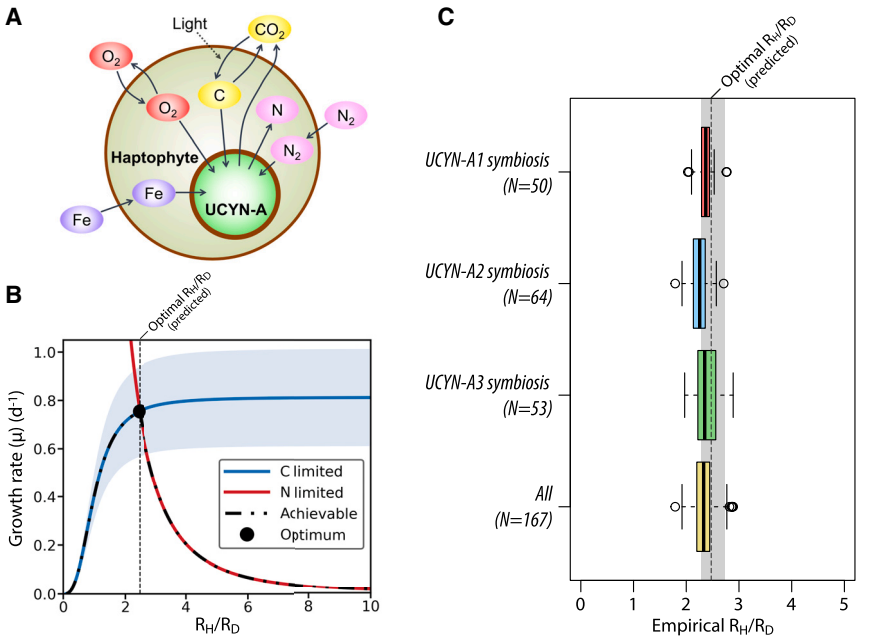


**Figure 2. The metabolic model predicts the optimal size ratio for the *B. bigelowii*/UCYN-A symbiosis**

(A) Conceptual view of resource acquisition and exchange in the *B. bigelowii*/UCYN-A symbiosis.

(B) Predicted growth rate of the symbiosis, $\mu$ ($d^{-1}$), vs. ratio of the effective spherical radii of the haptophyte and UCYN-A, $R_H/R_D$. The solid blue line indicates the predicted growth rate for the symbiotic pair when nothing limits the growth but the C provided through the haptophyte photosynthesis across different host-symbiont size ratios, and the blue shading indicates the range inferred by 1 standard deviation in the C-specific photosynthesis rate of haptophytes in this size range.[21] The red line is the modeled maximum growth rate when nothing limits the growth but the N provided by UCYN-A through $N_2$ fixation, calibrated by the maximum observed N-specific $N_2$ fixation rate in UCYN-A.[18] The lowest of these two growth rates is the achievable growth rate (black dash dotted line). The highest synchronized growth rate occurs at the radius ratio where the blue and red lines cross $(R_H/R_D)_{opt}$ (black circle).

(C) Distribution of the observed ratio of the radii of haptophyte cells and UCYN-A for each individual symbiotic pair within and across UCYN-A sublineages. N is the number of measured symbiotic pairs. The dashed vertical line and gray shading indicate the predicted optimal ratio from the model depicted in (B) and its range relative to one standard deviation in the empirical maximum photosynthesis rate.

See also Figure S2.

(optimization of fitness) under the physiological constraints imposed by the division of labor in resource acquisition and exchange. We formulated a mathematical model (depicted schematically in Figure 2A and detailed in STAR Methods), which assumes that the cell division rates of host and symbiont are synchronized,[22–24] that fixed C and N are supplied exclusively by the haptophyte and UCYN-A, respectively,[18] and that other elemental resources are not limiting. The diffusion of oxygen into UCYN-A from the interior of the haptophyte host, which can disable nitrogenase,[25] was assumed to be slowed by a hopanoid-containing membrane in UCYN-A.[26] The resulting $O_2$ flux into UCYN-A is assumed to be sufficient to sustain $N_2$ fixation and biosynthesis without leading to nitrogenase inactivation. We formulated ordinary differential equations to describe the rates of change of N and C cell-quotas in the symbiotic pair (STAR Methods). Sources from $N_2$ and C fixation are balanced by the reduction in quotas due to synchronized cell division. Assuming steady growth, the model predicts relationships between the potential growth rate if photosynthetic C acquisition is the limiting factor (here termed "C-limited growth rate," $\mu_C^{max}$, and $day^{-1}$) and the potential growth rate if $N_2$ fixation is the limiting factor (here termed "N-limited growth rate," $\mu_N^{max}$, and $day^{-1}$), each with respect to the ratio of the effective haptophyte cell and UCYN-A radii, $R_H/R_D$.

The modeled C-limited growth rate of the symbiosis (Figure 2B, blue line) increases steeply at low radius ratios, when the cost to the haptophyte of supporting the UCYN-A symbiont is high, and saturates when the haptophyte becomes sufficiently large that the C demand of UCYN-A is small relative to its own requirements. Conversely, N-limited growth (Figure 2B, red line) rapidly declines as the haptophyte-UCYN-A size ratio increases because a small diazotroph cannot fix $N_2$ sufficiently rapidly to supply both itself and a much larger host (STAR Methods). Note that the host/symbiont volume ratio (and associated mass demand) scales as the cube of the radius ratio, hence the steep gradients. The upper limits on C fixation by the haptophyte and $N_2$ fixation by UCYN-A are ultimately constrained by the maximum material investment in, and limiting turnover times of, the respective enzymes (STAR Methods).

For any given radius ratio, $R_H/R_D$, the achievable synchronized growth rate is either C- or N-limited, depending on whether the C-limited (Figure 2B, blue line) or N-limited (Figure 2B, red line) curve is lower. The achievable growth rate is indicated by the dot-dashed gray line in Figure 2B, exhibiting a maximum where the C- and N-limited limits cross (black dot and dashed vertical line, Figure 2B). If we associate the highest growth rate with maximum fitness, then the optimal radius ratio, $(R_H/R_D)_{opt}$, is located at this maximum. The position of this maximum can be directly solved from the model equations (STAR Methods)

$$(R_H/R_D)_{opt} = \left(\frac{N_N^{max}\,E}{P_C^{max}}\right)^{1/(3\beta)} \qquad \text{(Equation 1)}$$

where $P_C^{max}$ and $N_N^{max}$ ($day^{-1}$) are the respective, empirically constrained, maximum specific C and N fixation rates (STAR Methods, Figure S2, and Tables S2 and S3) and $\beta = 0.939$[27] is an empirical coefficient relating C quota and cell volume. $E$ (dimensionless) represents the cost of synthesizing biomass from inorganic substrates, evaluated from thermodynamic principles[28] (STAR Methods). The predicted optimal radius ratio, $(R_H/R_D)_{opt}$ = 2.47 (+0.27/−0.18) (Figure 2B and gray bar in

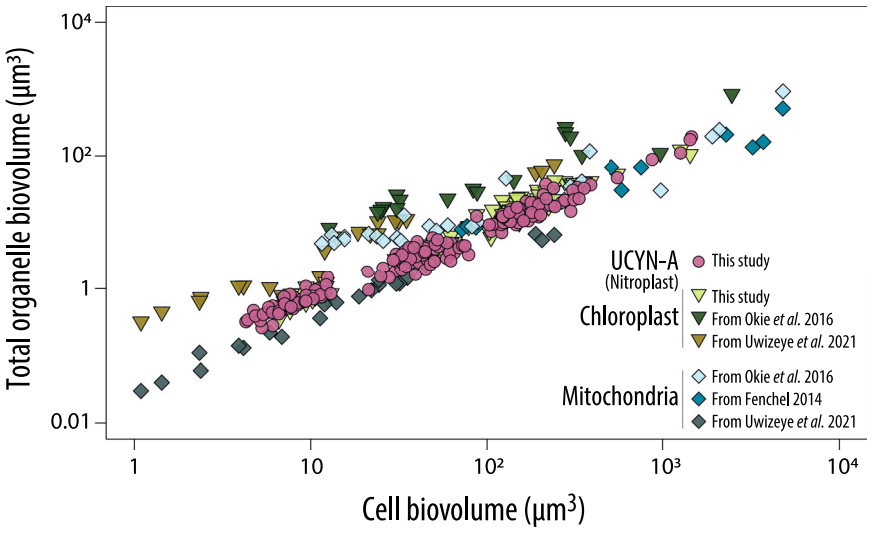


**Figure 3. UCYN-A volumetric scaling is consistent with that of organelles in protists**

Previously reported data of chloroplasts, mitochondria, and cell volumes for different species of protists are shown together with the UCYN-A and *B. bigelowii* volumes measured in this study (we refer the reader to the original references for a detailed list of the species included).

Figure 2C), is consistent with the highly conserved radius ratio observed in the *B. bigelowii*/UCYN-A symbiosis (2.33 ± 0.20; Figure 2C) and independent of the UCYN-A sublineage size. The predicted optimum ratio is robust to uncertainties in the parameter values (Figures S2A and S2B) and the possibility that UCYN-A supplements energy demand by light harvesting (Figures S2C and S2D) because of the steep and opposing gradients in C- and N-limited growth rates as a function of the radius ratio (Figures 2B and S2). In addition, it is generally accepted that haptophytes can be mixotrophic, i.e., they can take up dissolved organic substrates.[29–32] Therefore, it is likely that the *B. bigelowii*/UCYN-A symbiosis engages in some form of organoheterotrophy. We have incorporated mixotrophy in the model structure in order to evaluate the effect that mixotrophy could have on the predicted host-symbiont size ratio (Equations 10 and 11). Again, the predicted optimum size ratio is relatively invariant to the mode of nutrition, i.e., pure photoautotrophy vs. mixotrophy (i.e., photoautotrophy and organoheterotrophy), even if organoheterotrophy during mixotrophy accounts for a significant fraction of total nutrition (Figure S2E). The correspondence of predicted optimum $(R_H/R_D)_{opt}$ and observed radius ratio (2.47 [+0.27/−0.18] vs. 2.33 [SD = 0.20]) lends support to the hypothesis that the remarkably consistent size relationship reflects the underlying constraints of the symbiotic resource economy.

## Size evolution in a broader context

We note that a similarly tight size relationship also exists between the volume of *B. bigelowii* and the total chloroplast volume ($\log_{10}(V_{chloro}) = 1.1\ \log_{10}(V_{hapto}) - 1.2$, $R^2 = 0.97$, $p < 10^{-16}$, linear regression analysis; Figure 1B), such that the total UCYN-A volume and the total chloroplast volume of its haptophyte host also scale with a close-to-linear relationship ($\log_{10}(V_{UCYN\text{-}A}) = 0.9\ \log_{10}(V_{hapto}) + 0.01$, $R^2 = 0.94$, $p < 10^{-16}$, linear regression analysis; Figure 1B). Indeed, the observed constancy of $(R_H/R_D)_{opt}$ strongly resembles the power-law relationships observed between total organelle and cell volume for mitochondria and chloroplasts across a wide range of eukaryotic phytoplankton species[33–35] (Figure 3), which are isometric or hypoallometric. We hypothesize that cell-organelle size relationships, which to-date have not been unequivocally explained, are subject to similar resource economy constraints. For example, the size of a mitochondrion may be constrained by the maximum respiratory requirement to provide energy for the whole cell, and the investment in chloroplasts must be sufficient to provide C for optimized growth.[33,34] A recent study revealed preserved ratios between the total chloroplast and mitochondria volumes within cells across diverse unicellular phytoplankton species ($R^2 = 0.95$),[35] with intercept close to the origin, as did a tight regression between the total chloroplast and UCYN-A volumes (inset Figure 1B). This reflects predictable, balanced, and quantitative interdependencies between $CO_2$ fixation, photosynthesis, respiration, and $N_2$ fixation. Extending this logic, the similarity implies that UCYN-A is, in many regards, functioning as a $N_2$-fixing organelle, or "nitroplast." It also shares other characteristics with organelles, including an extremely reduced genome,[7] having lost at least three-quarters of the genes when compared with their free-living closest cyanobacterial relatives such as *Crocosphaera watsonii*.[36] As in mitochondrial and chloroplast genomes, UCYN-A lacks the methionyl-tRNA formyltransferase encoding (*fmt*) gene needed for the initiation of mRNA translation in bacteria.[37] The lack of the *fmt* gene in UCYN-A suggests that the haptophyte host might use the same mechanism to control mRNA translation in UCYN-A and in its mitochondria and chloroplasts. There is strong evidence showing the coordinated division of both UCYN-A and chloroplasts, which are subsequently vertically transmitted from the mother to the daughter algal cells,[6,22,24] which is also a common property of organelles.

Most $N_2$-fixing bacteria have mechanisms to regulate $N_2$ fixation when external sources of fixed N are available, thus alleviating the high energetic cost of this process.[38] Intriguingly, UCYN-A has lost the genes allowing this control[7] and, as a consequence, they fix $N_2$ gas into ammonium even in nutrient-rich environments.[18] Nitrate and ammonium are the most common N sources for phytoplankton growth.[39] However, natural populations of the UCYN-A/*B. bigelowii* symbiosis do not take up enough nitrate or ammonium from the environment to support their growth, relying on UCYN-A as their main source to meet their N demands,[18] just as they rely on their chloroplasts for fixed C. Hence, in the spectrum between symbionts and organelles, UCYN-A shares many characteristics with the latter, suggesting that it is well along an evolutionary path toward a nitroplast.

One might question why an $N_2$-fixing organelle-like entity has not yet evolved or is evolving so slowly compared with mitochondria and plastids. Although we cannot answer this question, we could speculate that at least the evolution of the *B. bigelowii*/UCYN-A symbiosis is based on recent events in a geological timescale. For example, ocean conditions on Earth during the mid to late Cretaceous, such as a warm tropical surface ocean and global anoxia,[40] together with the dominance of diazotrophic cyanobacteria[41] and *B. bigelowii* species turning into a more phagotrophic strategy to survive and recover from the end-Cretaceous darkness period caused after the bolide impact on Earth,[32] might have favored the encounter of $N_2$-fixers and eukaryotes. Accordingly, not only did the *B. bigelowii*/UCYN-A symbiosis originate ca. 91 mya,[42] i.e., in the late Cretaceous, but also the origin of other marine (e.g., marine planktonic diatom diazotroph associations[43]) and non-marine (e.g., plants with specialized root organs [nodules] where $N_2$-fixing bacteria are hosted[44]) $N_2$-fixing symbioses have been dated to the Cretaceous period.

Overall, our study shows that the size relationship of the $N_2$-fixing cyanobacterium UCYN-A with *B. bigelowii* is determined by fundamental constraints rooted in the exchange of resources between symbiotic partners, i.e., in a coordinated metabolism. UCYN-A and other $N_2$-fixing spheroid bodies[45–47] are "snapshots" along the spectrum of the evolution of bacterial-derived organelles in eukaryotes. However, how far along this trajectory these $N_2$-fixing spheroid bodies are will ultimately be uncovered by the demonstration of additional organelle properties, such as the coordination of protein import and export.

### Limitations of the study

This study does not unequivocally demonstrate that UCYN-A is an organelle for $N_2$ fixation because, in order to do so, additional experiments would be necessary to show, for instance, protein trafficking and/or gene migration between both symbiotic partners, i.e., UCYN-A and *B. bigelowii*. Moreover, the symbiotic relationship between the UCYN-A2 sublineage and *B. bigelowii* might be occasionally unstable under undetermined culture conditions, as it has been reported in this and other similar difficult-to-grow $N_2$-fixing symbioses.[6,47] Identifying the conditions triggering the instability of these types of symbioses might help us to better understand what makes them stay together in the natural environment. Furthermore, knowing whether UCYN-A can or cannot be cultivated as a free-living population would be very informative in respect of its nature. In this regard, attempts to maintain free-living UCYN-A cells have been unsuccessful so far, supporting the nitroplast hypothesis, yet further attempts are needed to confirm this observation.

## STAR★METHODS

Detailed methods are provided in the online version of this paper and include the following:

- KEY RESOURCES TABLE
- RESOURCE AVAILABILITY
  - Lead contact
  - Materials availability
  - Data and code availability
- EXPERIMENTAL MODEL AND STUDY PARTICIPANT DETAILS
  - Microbe strains
- METHOD DETAILS
  - Sampling, visualization, and volumetric estimation of *B. bigelowii*/UCYN-A symbioses collected from the diverse marine locations
  - A model of carbon and nitrogen economy of the *B. bigelowii*/UCYN-A symbiosis
  - Maximum photosynthetic rate
  - Measured specific $N_2$ fixation rates
- QUANTIFICATION AND STATISTICAL ANALYSIS

## SUPPLEMENTAL INFORMATION

Supplemental information can be found online at https://doi.org/10.1016/j.cell.2024.02.016.

## ACKNOWLEDGMENTS

We thank Clara Ruiz-González, Kendra A. Turk-Kubo, and Ana M. Cabello for their helpful comments and Wing Kwan Esther Mak and Kyoko Hagino for providing images of the *B. bigelowii*/UCYN-A2 symbiosis. M.J.F. thanks Chris Follett and Mydia Phan for stimulating and helpful discussions. F.M.C.-C. was supported by grants from the Spanish Ministry of Science and Innovation ("Ramón y Cajal" fellowship; RYC2021-032949-I), "La Caixa" Foundation (grant 105090, UCYNELLE project), and the European Union's Horizon 2020 research and innovation program under the Marie Skłodowska-Curie grant agreement (grant 749380, UCYN2PLAST project). This work acknowledges the Severo Ochoa Centre of Excellence accreditation (CEX2019-000928-S) funded by AEI 10.13039/501100011033 and grants from the Simons Foundation (Life Sciences 544338 and LS-ECIAMEE-00001549 to K.I. and 824082 to J.P.Z., SCOPE 724220 to J.P.Z. and 721248 to M.J.F., and CBIOMES 549931 to M.J.F.).

## AUTHOR CONTRIBUTIONS

Conceptualization, F.M.C.-C., K.I., J.P.Z., and M.J.F.; methodology, F.M.C.-C., K.I., J.P.Z., and M.J.F.; investigation, F.M.C.-C., K.I., J.P.Z., and M.J.F.; visualization, F.M.C.-C., K.I., and M.J.F.; funding acquisition, F.M.C.-C., K.I., J.P.Z., and M.J.F.; writing – original draft, F.M.C.-C., K.I., J.P.Z., and M.J.F.; writing – review & editing, F.M.C.-C., K.I., J.P.Z., and M.J.F.

## DECLARATION OF INTERESTS

The authors declare no competing interests.

Received: April 12, 2023
Revised: October 6, 2023
Accepted: February 14, 2024
Published: March 11, 2024

## REFERENCES

1. Foster, R.A., and Zehr, J.P. (2019). Diversity, genomics, and distribution of phytoplankton-cyanobacterium single-cell symbiotic associations. Annu. Rev. Microbiol. *73*, 435–456.
2. Thompson, A.W., Foster, R.A., Krupke, A., Carter, B.J., Musat, N., Vaulot, D., Kuypers, M.M.M., and Zehr, J.P. (2012). Unicellular cyanobacterium symbiotic with a single-celled eukaryotic alga. Science *337*, 1546–1550.
3. Zehr, J.P., and Capone, D.G. (2020). Changing perspectives in marine nitrogen fixation. Science *368*, eaay9514.

4. Rai, A.N., Söderbäck, E., and Bergman, B. (2000). Tansley Review No. 116: Cyanobacterium-plant symbioses. New Phytol. *147*, 449–481.
5. Hagino, K., Onuma, R., Kawachi, M., and Horiguchi, T. (2013). Discovery of an endosymbiotic nitrogen-fixing cyanobacterium UCYN-A in *Braarudosphaera bigelowii* (Prymnesiophyceae). PLoS One *8*, e81749.
6. Suzuki, S., Kawachi, M., Tsukakoshi, C., Nakamura, A., Hagino, K., Inouye, I., and Ishida, K.I. (2021). Unstable relationship between *Braarudosphaera bigelowii* (= *Chrysochromulina parkeae*) and its nitrogen-fixing endosymbiont. Front. Plant Sci. *12*, 749895.
7. Tripp, H.J., Bench, S.R., Turk, K.A., Foster, R.A., Desany, B.A., Niazi, F., Affourtit, J.P., and Zehr, J.P. (2010). Metabolic streamlining in an open-ocean nitrogen-fixing cyanobacterium. Nature *464*, 90–94.
8. Green, J.C., and Leadbeater, B.S.C. (1972). Chrysochromulina Parkeae Sp.Nov. [Haptophyceae] a New Species Recorded From S.W. England and Norway. J. Mar. Biol. Ass. *52*, 469–474.
9. Hagino, K., Tomioka, N., Young, J.R., Takano, Y., Onuma, R., and Horiguchi, T. (2016). Extracellular calcification of *Braarudosphaera bigelowii* deduced from electron microscopic observations of cell surface structure and elemental composition of pentaliths. Mar. Micropaleontol. *125*, 85–94.
10. Farnelid, H., Turk-Kubo, K., Muñoz-Marín, M.C., and Zehr, J.P. (2016). New insights into the ecology of the globally significant uncultured nitrogen-fixing symbiont UCYN-A. Aquat. Microb. Ecol. *77*, 125–138.
11. Cornejo-Castillo, F.M., Muñoz-Marín, M.C., Turk-Kubo, K.A., Royo-Llonch, M., Farnelid, H., Acinas, S.G., and Zehr, J.P. (2019). UCYN-A3, a newly characterized open ocean sublineage of the symbiotic $N_2$-fixing cyanobacterium *Candidatus* Atelocyanobacterium thalassa. Environ. Microbiol. *21*, 111–124.
12. Cabello, A.M., Turk-Kubo, K.A., Hayashi, K., Jacobs, L., Kudela, R.M., and Zehr, J.P. (2020). Unexpected presence of the nitrogen-fixing symbiotic cyanobacterium UCYN-A in Monterey Bay, California. J. Phycol. *56*, 1521–1533.
13. Finkel, Z.V. (2001). Light absorption and size scaling of light-limited metabolism in marine diatoms. Limnol. Oceanogr. *46*, 86–94.
14. Niklas, K.J., and Enquist, B.J. (2001). Invariant scaling relationships for interspecific plant biomass production rates and body size. Proc. Natl. Acad. Sci. USA *98*, 2922–2927.
15. Marañón, E., Cermeño, P., Rodríguez, J., Zubkov, M.V., and Harris, R.P. (2007). Scaling of phytoplankton photosynthesis and cell size in the ocean. Limnol. Oceanogr *52*, 2190–2198.
16. Marañón, E., Cermeño, P., López-Sandoval, D.C., Rodríguez-Ramos, T., Sobrino, C., Huete-Ortega, M., Blanco, J.M., and Rodríguez, J. (2013). Unimodal size scaling of phytoplankton growth and the size dependence of nutrient uptake and use. Ecol. Lett. *16*, 371–379.
17. Aloisi, G. (2015). Covariation of metabolic rates and cell size in coccolithophores. Biogeosciences *12*, 4665–4692.
18. Mills, M.M., Turk-Kubo, K.A., van Dijken, G.L., Henke, B.A., Harding, K., Wilson, S.T., Arrigo, K.R., and Zehr, J.P. (2020). Unusual marine cyanobacteria/haptophyte symbiosis relies on $N_2$ fixation even in N-rich environments. ISME J. *14*, 2395–2406.
19. Krupke, A., Musat, N., LaRoche, J., Mohr, W., Fuchs, B.M., Amann, R.I., Kuypers, M.M.M., and Foster, R.A. (2013). In situ identification and $N_2$ and C fixation rates of uncultivated cyanobacteria populations. Syst. Appl. Microbiol. *36*, 259–271.
20. Devassy, R.P., El-Sherbiny, M.M., Al-Sofyani, A.A., Crosby, M.P., and Al-Aidaroos, A.M. (2019). Seasonality and latitudinal variability in the diatom-cyanobacteria symbiotic relationships in the coastal waters of the Red Sea, Saudi Arabia. Symbiosis *78*, 215–227.
21. Taniguchi, D.A.A., Franks, P.J.S., and Poulin, F.J. (2014). Planktonic biomass size spectra: an emergent property of size-dependent physiological rates, food web dynamics, and nutrient regimes. Mar. Ecol. Prog. Ser. *514*, 13–33.
22. Muñoz-Marín, M.C., Shilova, I.N., Shi, T., Farnelid, H., Cabello, A.M., and Zehr, J.P. (2019). The transcriptional cycle is suited to daytime $N_2$ fixation in the unicellular cyanobacterium "*Candidatus* atelocyanobacterium thalassa" (UCYN-A). mBio *10*, e02495-18.
23. Landa, M., Turk-Kubo, K.A., Cornejo-Castillo, F.M., Henke, B.A., and Zehr, J.P. (2021). Critical role of light in the growth and activity of the marine $N_2$-fixing UCYN-A symbiosis. Front. Microbiol. *12*, 666739.
24. Cabello, A.M., Cornejo-Castillo, F.M., Raho, N., Blasco, D., Vidal, M., Audic, S., De Vargas, C., Latasa, M., Acinas, S.G., and Massana, R. (2016). Global distribution and vertical patterns of a prymnesiophyte-cyanobacteria obligate symbiosis. ISME J. *10*, 693–706.
25. Oelze, J. (2000). Respiratory protection of nitrogenase in *Azotobacter* species: is a widely held hypothesis unequivocally supported by experimental evidence? FEMS Microbiol. Rev. *24*, 321–333.
26. Cornejo-Castillo, F.M., and Zehr, J.P. (2019). Hopanoid lipids may facilitate aerobic nitrogen fixation in the ocean. Proc. Natl. Acad. Sci. USA *116*, 18269–18271.
27. Menden-Deuer, S., and Lessard, E.J. (2000). Carbon to volume relationships for dinoflagellates, diatoms, and other protist plankton. Limnol. Oceanogr. *45*, 569–579.
28. Rittmann, B.E., and McCarty, P.L. (2001). 2.7 Yield coefficient and reaction energetics and Table 2.3 Organic half-reactions and their Gibb's free energy. In Environmental Biotechnology: Principles and Applications (McGraw-Hill), pp. 136–137. 155–159.
29. Frias-Lopez, J., Thompson, A., Waldbauer, J., and Chisholm, S.W. (2009). Use of stable isotope-labelled cells to identify active grazers of picocyanobacteria in ocean surface waters. Environ. Microbiol. *11*, 512–525.
30. Unrein, F., Gasol, J.M., Not, F., Forn, I., and Massana, R. (2014). Mixotrophic haptophytes are key bacterial grazers in oligotrophic coastal waters. ISME J. *8*, 164–176.
31. Dölger, J., Nielsen, L.T., Kiørboe, T., and Andersen, A. (2017). Swimming and feeding of mixotrophic biflagellates. Sci. Rep. *7*, 39892.
32. Gibbs, S.J., Bown, P.R., Ward, B.A., Alvarez, S.A., Kim, H., Archontikis, O.A., Sauterey, B., Poulton, A.J., Wilson, J., and Ridgwell, A. (2020). Algal plankton turn to hunting to survive and recover from end-Cretaceous impact darkness. Sci. Adv. *6:eabc9123*.
33. Fenchel, T. (2014). Respiration in heterotrophic unicellular eukaryotic organisms. Protist *165*, 485–492.
34. Okie, J.G., Smith, V.H., and Martin-Cereceda, M. (2016). Major evolutionary transitions of life, metabolic scaling and the number and size of mitochondria and chloroplasts. Proc. Biol. Sci. *283*, 20160611.
35. Uwizeye, C., Decelle, J., Jouneau, P.H., Flori, S., Gallet, B., Keck, J.B., Bo, D.D., Moriscot, C., Seydoux, C., Chevalier, F., et al. (2021). Morphological bases of phytoplankton energy management and physiological responses unveiled by 3D subcellular imaging. Nat. Commun. *12*, 1049.
36. Bench, S.R., Heller, P., Frank, I., Arciniega, M., Shilova, I.N., and Zehr, J.P. (2013). Whole genome comparison of six *Crocosphaera watsonii* strains with differing phenotypes. J. Phycol. *49*, 786–801.
37. Gualerzi, C.O., and Pon, C.L. (2015). Initiation of mRNA translation in bacteria: Structural and dynamic aspects. Cell. Mol. Life Sci. *72*, 4341–4367.
38. Dixon, R., and Kahn, D. (2004). Genetic regulation of biological nitrogen fixation. Nat. Rev. Microbiol. *2*, 621–631.
39. Glibert, P.M., Wilkerson, F.P., Dugdale, R.C., Raven, J.A., Dupont, C.L., Leavitt, P.R., Parker, A.E., Burkholder, J.M., and Kana, T.M. (2016). Pluses and minuses of ammonium and nitrate uptake and assimilation by phytoplankton and implications for productivity and community composition, with emphasis on nitrogen-enriched conditions. Limnol. Oceanogr. *61*, 165–197.
40. Wilson, P.A., and Norris, R.D. (2001). Warm tropical ocean surface and global anoxia during the mid-Cretaceous period. Nature *412*, 425–429.
41. Kashiyama, Y., Ogawa, N.O., Kuroda, J., Shiro, M., Nomoto, S., Tada, R., Kitazato, H., and Ohkouchi, N. (2008). Diazotrophic cyanobacteria as the major photoautotrophs during mid-Cretaceous oceanic anoxic events: Nitrogen and carbon isotopic evidence from sedimentary porphyrin. Org. Geochem. *39*, 532–549.

42. Cornejo-Castillo, F.M., Cabello, A.M., Salazar, G., Sánchez-Baracaldo, P., Lima-Mendez, G., Hingamp, P., Alberti, A., Sunagawa, S., Bork, P., DeVargas, C., et al. (2016). Cyanobacterial symbionts diverged in the late Cretaceous towards lineage-specific nitrogen fixation factories in single-celled phytoplankton. Nat. Commun. *7*, 11071.

43. Caputo, A., Nylander, J.A.A., and Foster, R.A. (2019). The genetic diversity and evolution of diatom-diazotroph associations highlights traits favoring symbiont integration. FEMS Microbiol. Lett. *366:fny297*.

44. van Velzen, R., Doyle, J.J., and Geurts, R. (2019). A resurrected scenario: Single gain and massive loss of nitrogen-fixing nodulation. Trends Plant Sci. *24*, 49–57.

45. Prechtl, J., Kneip, C., Lockhart, P., Wenderoth, K., and Maier, U.G. (2004). Intracellular spheroid bodies of *Rhopalodia gibba* have nitrogen-fixing apparatus of cyanobacterial origin. Mol. Biol. Evol. *21*, 1477–1481.

46. Nakayama, T., Kamikawa, R., Tanifuji, G., Kashiyama, Y., Ohkouchi, N., Archibald, J.M., and Inagaki, Y. (2014). Complete genome of a nonphotosynthetic cyanobacterium in a diatom reveals recent adaptations to an intracellular lifestyle. Proc. Natl. Acad. Sci. USA *111*, 11407–11412.

47. Schvarcz, C.R., Wilson, S.T., Caffin, M., Stancheva, R., Li, Q., Turk-Kubo, K.A., White, A.E., Karl, D.M., Zehr, J.P., and Steward, G.F. (2022). Overlooked and widespread pennate diatom-diazotroph symbioses in the sea. Nat. Commun. *13*, 799.

48. Ryabov, A., Kerimoglu, O., Litchman, E., Olenina, I., Roselli, L., Basset, A., Stanca, E., and Blasius, B. (2021). Shape matters: the relationship between cell geometry and diversity in phytoplankton. Ecol. Lett. *24*, 847–861.

49. Robson, R.L., and Postgate, J.R. (1980). Oxygen and hydrogen in biological nitrogen fixation. Annu. Rev. Microbiol. *34*, 183–207.

50. Poole, R.K., and Hill, S. (1997). Respiratory protection of nitrogenase activity in Azotobacter vinelandii–roles of the terminal oxidases. Biosci. Rep. *17*, 303–317.

51. Martínez-Pérez, C., Mohr, W., Löscher, C.R., Dekaezemacker, J., Littmann, S., Yilmaz, P., Lehnen, N., Fuchs, B.M., Lavik, G., Schmitz, R.A., et al. (2016). The small unicellular diazotrophic symbiont, UCYN-A, is a key player in the marine nitrogen cycle. Nat. Microbiol. *1*, 16163.

52. Verity, P.G., Robertson, C.Y., Tronzo, C.R., Andrews, M.G., Nelson, J.R., and Sieracki, M.E. (1992). Relationships between cell volume and the carbon and nitrogen content of marine photosynthetic nanoplankton. Limnol. Oceanogr. *37*, 1434–1446.

53. Strathmann, R.R. (1967). Estimating the organic carbon content of phytoplankton from cell volume or plasma volume. Limnol. Oceanogr. *12*, 411–418.

54. Inomura, K., Follett, C.L., Masuda, T., Eichner, M., Prášil, O., and Deutsch, C. (2020). Carbon transfer from the host diatom enables fast growth and high rate of $N_2$ fixation by symbiotic heterocystous cyanobacteria. Plants (Basel) *9*, 192.

55. LaRoche, J., and Breitbarth, E. (2005). Importance of the diazotrophs as a source of new nitrogen in the ocean. J. Sea Res. *53*, 67–91.

56. Großkopf, T., and LaRoche, J. (2012). Direct and indirect costs of dinitrogen fixation in *Crocosphaera watsonii* WH8501 and possible implications for the nitrogen cycle. Front. Microbiol. *3*, 236.

57. Dron, A., Rabouille, S., Claquin, P., Le Roy, B., Talec, A., and Sciandra, A. (2012). Light-dark (12:12) cycle of carbon and nitrogen metabolism in *Crocosphaera watsonii* WH8501: relation to the cell cycle. Environ. Microbiol. *14*, 967–981.

58. Foster, R.A., Kuypers, M.M.M., Vagner, T., Paerl, R.W., Musat, N., and Zehr, J.P. (2011). Nitrogen fixation and transfer in open ocean diatom-cyanobacterial symbioses. ISME J. *5*, 1484–1493.

59. Lichtl, R.R., Bazin, M.J., and Hall, D.O. (1997). The biotechnology of hydrogen production by *Nostoc flagelliforme* grown under chemostat conditions. Appl. Microbiol. Biotechnol. *47*, 701–707.

60. Kuhla, J., and Oelze, J. (1988). Dependency of growth yield, maintenance and $K_s$-values on the dissolved oxygen concentration in continuous cultures of *Azotobacter vinelandii*. Arch. Microbiol. *149*, 509–514.

61. Villareal, T.A. (1992). Marine nitrogen fixing diatom–cyanobacteria symbioses. In Marine Pelagic Cyanobacteria: Trichodesmium and other Diazotrophs, E.J. Carpenter, D.G. Carpone, and J.G. Rueter, eds. (Dordrecht: Springer Netherlands), pp. 163–175.

62. Villareal, T.A. (1990). Laboratory culture and preliminary characterization of the nitrogen-fixing *Rhizosolenia-Richelia* symbiosis. Mar. Ecol. *11*, 117–132.

63. Inomura, K., Bragg, J., and Follows, M.J. (2017). A quantitative analysis of the direct and indirect costs of nitrogen fixation: a model based on *Azotobacter vinelandii*. ISME J. *11*, 166–175.

## STAR★METHODS

### KEY RESOURCES TABLE

| REAGENT or RESOURCE | SOURCE | IDENTIFIER |
|---|---|---|
| Chemicals, peptides, and recombinant proteins | | |
| DAPI (4′,6-diamidino-2-phenylindole) | ThermoFisher | Cat# 62247 |
| Alexa Fluor™ 488 | ThermoFisher | Cat# B40953 |
| Alexa Fluor™ 594 | ThermoFisher | Cat# B40957 |
| Deposited data | | |
| Code (Cell Flux Model of UCYN-A: CFM_UCYN-A) | GitHub/Zenodo | https://zenodo.org/record/5057366 |
| Oligonucleotides | | |
| UPRYM69 (probe linked with the enzyme horseradish peroxidase (HRP) targeting the haptophyte host of the UCYN-A1 sublineage): CACATAGGAACATCCTCC | Cornejo-Castillo et al.[42] | N/A |
| UPRYM69 competitor: CACATTGGAACATCCTCC | Cornejo-Castillo et al.[42] | N/A |
| UBRADO69 (probe linked with the enzyme HRP targeting *B. bigelowii* the haptophyte host of the UCYN-A2 sublineage): CACATTGGAACATCCTCC | Cornejo-Castillo et al.[42] | N/A |
| UBRADO69 competitor: CACATAGGAACATCCTCC | Cornejo-Castillo et al.[42] | N/A |
| Helper A-PRYM (targets *Haptophyta*): GAAAGGTGCTGAAGGAGT | Cornejo-Castillo et al.[42] | N/A |
| Helper B-PRYM (targets *Haptophyta*): AATCCCTAGTCGGCATGG | Cornejo-Castillo et al.[42] | N/A |
| UCYN–A1-732 (probe linked with the enzyme HRP targeting the UCYN-A1 sublineage): GTTACGGTCCAGTAGCAC | Krupke et al.[19] | N/A |
| UCYN-A1-732 competitor: GTTGCGGTCCAGTAGCAC | Cornejo-Castillo et al.[42] | N/A |
| UCYN–A2-732 (probe linked with the enzyme HRP targeting the UCYN-A2 sublineage): GTTGCGGTCCAGTAGCAC | Cornejo-Castillo et al.[42] | N/A |
| UCYN-A2-732 competitor: GTTACGGTCCAGTAGCAC | Krupke et al.[19] | N/A |
| Helper A-UCYN-A-732 (targets UCYN-A): GCCTTCGCCACCGATGTTCTT | Krupke et al.[19] | N/A |
| Helper B-UCYN-A-732 (targets UCYN-A): AGCTTTCGTCCCTGAGTGTCA | Krupke et al.[19] | N/A |
| UCYN-A2-1137 (probe linked with the enzyme HRP targeting the UCYN-A2 sublineage): CTTCCTAAAGTGCCCACCTT | Cornejo-Castillo et al.[11] | N/A |
| UCYN-A3-1137 (probe linked with the enzyme HRP targeting the UCYN-A3 sublineage): CTTCCTAGAGTGCCCACCTT | Cornejo-Castillo et al.[11] | N/A |
| Helper UCYN-A2A3 (targets UCYN-A): CGGTTTGTCACCGGCAGT | Cornejo-Castillo et al.[11] | N/A |
| Software and algorithms | | |
| Carl Zeiss™ AxioVision Rel. 4.8.2 Software | Fisher Scientific | Cat# 11875113 |
| R Studio; ‘stats’ R package | R Core Team (2019) | https://www.R-project.org/; RRID: SCR_001905 |

## RESOURCE AVAILABILITY

### Lead contact

Further information and requests for resources and reagents should be directed to and will be fulfilled by the lead contact, Francisco M. Cornejo-Castillo (fmcornejo@icm.csic.es).

### Materials availability

This study did not generate new unique reagents.

### Data and code availability

- All raw microscopy data reported in this paper will be shared by the lead contact upon request.
- The model code of carbon and nitrogen economy in the *B. bigelowii*/UCYN-A symbiosis is available from GitHub/Zenodo (https://doi.org/10.5281/zenodo.5057366), listed in key resources table.
- Any additional information required to reanalyze the data reported in this paper is available from the lead contact upon request.

## EXPERIMENTAL MODEL AND STUDY PARTICIPANT DETAILS

### Microbe strains

All the specimens of the different strains of the *B. bigelowii*/UCYN-A symbiosis analyzed in this study came from natural seawater samples (see method details), and they were detected and distinguished from the rest of the environmental microbial community using the probes listed in the key resources table.

## METHOD DETAILS

### Sampling, visualization, and volumetric estimation of *B. bigelowii*/UCYN-A symbioses collected from the diverse marine locations

In order to capture and measure the wide range of sizes of the *B. bigelowii*/UCYN-A symbiosis, we analyzed a diverse set of environmental samples in which the presence of the *B. bigelowii*/UCYN-A symbiosis had previously been reported using CAtalyzed Reporter Deposition Fluorescence In Situ Hybridization (CARD-FISH) as detailed in,[11,12] including UCYN-A symbionts of the UCYN-A1, UCYN-A2 and UCYN-A3 sublineages.[11,12] These samples had been collected from the Scripps Institution of Oceanography (SIO) Ellen Browning Scripps Memorial Pier (32° 52' 1.7'' N, 117° 15' 27.3'' W, at 1 meter depth in July 2015) in La Jolla, CA (USA), from Station ALOHA in the North Pacific Ocean (22° 45' N, 158° W, at 45 meters depth in April 2015) and from the Santa Cruz Municipal Wharf, Santa Cruz, CA (USA) (SCMW; 36° 57' 28.7136'' N, 122° 01' 03.2124'' W, at 1 meter depth in September 2018).[11,12] Samples from Scripps contained mostly UCYN-A1 and UCYN-A2, whereas samples from Station ALOHA were dominated by UCYN-A1 and UCYN-A3 symbionts.[11] Samples from SCMW mainly contained UCYN-A2 symbionts.[12] In all cases, a double CARD-FISH hybridization with specific probes in combination with helpers and competitors for the UCYN-A1, UCYN-A2 and UCYN-A3 sublineages and their corresponding haptophyte hosts allowed the identification of the *B. bigelowii*/UCYN-A symbiosis[11,12] (see probes, competitors, and helpers in Cornejo-Castillo et al.[11] and in the key resources table). A filter section from each sample was inspected under epifluorescence on a Zeiss Axioplan epifluorescence microscope (Oberkochen, Germany) equipped with digital imaging, and micrographs were taken under ultraviolet (DAPI signal of the DNA), blue (green labeled haptophyte (host) cell with Alexa 488 stain), and green (red labeled UCYN-A (symbiont) with Alexa 594 stain) excitation wavelengths (Figure 1C). Micrographs were analyzed with the Carl Zeiss™ AxioVision Rel. 4.8.2 Software, which allowed us to delimit the contour of positive labeled haptophyte/UCYN-A symbioses, measure their sizes and estimate their volumes. These measurements included the length (μm) and width (μm) of haptophyte cells, area ($\mu m^2$) and width (μm) of one of their two chloroplasts, and the diameter (μm) of UCYN-A for a total of 167 identified symbiotic partnerships (Table S1). We used these measurements to estimate the volume ($\mu m^3$) of the haptophyte cells, their chloroplasts and UCYN-A. In order to calculate the volume of haptophyte cells, we assumed the cell geometry of an ellipsoid as indicated in,[48] and applied the corresponding formula. The same geometry was assumed for chloroplasts based on our direct visual inspection of the filters. However, we only could estimate the volume of chloroplasts in 108 cells because sometimes the orientation of the cell on the filter did not allow us to visualize and measure them. The geometry of UCYN-A was assumed to be a sphere based on our visual inspection and, therefore, the formula of the volume of a sphere was applied to estimate the volume of UCYN-A.

### A model of carbon and nitrogen economy of the *B. bigelowii*/UCYN-A symbiosis

To explore the constraints of the host-symbiont cell size ratio, we have developed a mechanistic model of the *B. bigelowii*/UCYN-A symbiosis (Cell Flux Model of UCYN-A: CFM_UCYN-A; see key resources table). We define the carbon quotas (mol C $pair^{-1}$) of the host and symbiont, $Q_{C,H}$ and $Q_{C,D}$ respectively, and the sum, $Q_C = Q_{C,H} + Q_{C,D}$. (Symbols are defined in Table S2). The time dependence of $Q_C$ (mol C $pair^{-1}$) can be expressed as follows:

$$\frac{dQ_C}{dt} = P_H - \mu Q_C(1+\varepsilon) - \gamma N_D \quad \text{(Equation 2)}$$

The first term on the right, $P_H$, is the rate of photosynthesis by the haptophyte (mol C pair$^{-1}$ d$^{-1}$). The second term on the right represents the investment of carbon in growth where $\mu$ is the synchronized growth rate (d$^{-1}$) and the non-dimensional factor $\varepsilon$ is the respiratory cost of ammonia-based synthesis of average cellular biomass. (Parameter values are given in Table S3). The third term represents the cost of $N_2$ fixation, where $N_D$ is the rate of $N_2$ fixation by the diazotroph (mol N pair$^{-1}$ d$^{-1}$), and $\gamma$ is the cost to reduce $N_2$ to ammonia (mol C mol N$^{-1}$). Values of $\gamma$ and $\varepsilon$ are estimated from redox and thermodynamic considerations. We assume that additional respiration to protect nitrogenase from interference by intra-cellular oxygen[49,50] is negligible due to the formation of a protective hopanoid barrier.[11] We are considering maximum growth rates and, for that circumstance, we assume that maintenance respiration costs are negligible. Similarly, we describe the rate of change of the total nitrogen quota of the pair as

$$\frac{dQ_N}{dt} = N_D - \mu Q_C Y^{NC} \quad \text{(Equation 3)}$$

Here, $Q_N = Q_{N,H} + Q_{N,D}$ is the nitrogen quota of the pair (mol N pair$^{-1}$). The first term on the right represents $N_2$ fixation by UCYN-A, which provides all the nitrogen for both partners, and the second term is the dilution of cellular nitrogen quota by synchronized division. $Y^{NC}$ is the collective elemental ratio (N:C) of the host and diazotroph (mol N (mol C)$^{-1}$), which has been empirically evaluated to be 6.3 ± 0.4.[51]

### Carbon-limited growth

For the case where photosynthesis is limiting, solving (Equation 2) and (Equation 3) at steady state and eliminating $N_D$, we find an expression for the maximum carbon-limited growth rate, $\mu_C^{max}$ (d$^{-1}$):

$$\mu_C^{max} = \frac{P_H^{max}}{Q_C E} \quad \text{(Equation 4)}$$

The dimensionless factor $E = (1 + \varepsilon + \gamma Y^{NC})$ represents the investment in, and energetic cost of, synthesizing one unit of "biomass" from inorganic carbon and dinitrogen gas. $P_H^{max}$ represents the maximum possible rate of cellular carbon fixation by the haptophyte.

Empirical data indicates that over the range of relevant haptophyte cell sizes, the maximum carbon specific rate of carbon fixation, $P_C^{max}$ (mol C (mol C)$^{-1}$ d$^{-1}$), falls between ~0.1-0.2 h$^{-1}$ without any significant allometric trend,[16] consistent with a compilation of maximum growth rate data[21] (Figures S3A and S3B). Thus, with constant $P_C^{max}$, the maximum photosynthetic rate, $P_H^{max} = P_C^{max} Q_{C,H}$ (mol C pair$^{-1}$ d$^{-1}$) scales linearly with cellular carbon quota. Using the observed relationship between the cellular C quota and cell volume,[27] $Q_{C,i} = \alpha V_i^{\beta}$, where $V_i$ is cell volume (μm$^3$), $\alpha$ (mol C μm$^{-3}$) and $\beta$ (dimensionless) are constants,[27] and subscript $i$ represents haptophyte ($H$) or UCYN-A ($D$) respectively. For spherical cells, $V_i = \frac{4}{3}\pi R_i^3$ and we obtain a simple expression for the maximum carbon-limited growth rate of the pair in terms of the ratio of the haptophyte and UCYN-A cell radii, $R_i$,

$$\mu_C^{max} = \frac{P_C^{max}}{E} \frac{\left(\frac{R_H}{R_D}\right)^{3\beta}}{\left(\frac{R_H}{R_D}\right)^{3\beta} + 1} \quad \text{(Equation 5)}$$

When the haptophyte is much larger than UCYN-A, $R_H \gg R_D$, $\mu_C^{max}$ asymptotes to an upper limit in which the carbon demand of UCYN-A is negligible and the photosynthetic carbon supply matches the demand of the haptophyte (Figure 2B; blue line). When the haptophyte is smaller than UCYN-A, $R_H \ll R_D$, $\mu_C^{max}$ is proportional to the ratio of the cell volumes (Figure 2B; blue line), reflecting the significance of the photosynthetic cost of the carbon demand for UCYN-A. In short, under photosynthetic carbon-limitation, the growth rate of the symbiotic pair is maximized when the haptophyte-UCYN-A size ratio is maximal.

### Nitrogen-limited growth

Conversely, nitrogen-limited growth favors a small haptophyte-UCYN-A size ratio. Assuming steady-state again (i.e., left hand side of (Equation 3) = 0), the maximum nitrogen-limited, synchronized growth rate can be expressed as a function of the maximum $N_2$ fixation rate of UCYN-A ($N_D^{max}$, mol N pair$^{-1}$ day$^{-1}$) and the nitrogen demand of the pair ($Q_C Y^{NC}$, mol N pair$^{-1}$):

$$\mu_N^{max} = \frac{N_D^{max}}{Q_C Y^{NC}} \quad \text{(Equation 6)}$$

This is the *maximum* nitrogen-specific $N_2$ fixation rate for the symbiotic pair. Here $N_2$ fixation rate per host-symbiont pair, $N_D^{max}$, is calibrated by the highest single cell specific rate observed in an individual UCYN-A cell, $N_N^{max}$ = 10.42 day$^{-1}$,[18] which is consistent with the highest rates observed in several other $N_2$-fixing cyanobacteria (Details in "Measured specific $N_2$ fixation rates" below, and Figure S3C). We calibrate the maximum per-cell $N_2$ fixation rate, $N_D^{max}$, with the observed maximum specific $N_2$ fixation rate for UCYN-A, $N_N^{max}$, as follows:

$$N_D^{max} = N_N^{max} Q_{C,D} Y^{NC} \quad \text{(Equation 7)}$$

Here $Y^{NC}$ for UCYN-A is assumed the same as that of the symbiotic pair, and the maximum per-cell $N_2$ fixation rate is proportional to the size of the spheroid body; i.e., the maximum per-cell quota of $N_2$ fixing enzymes increasing with cell volume and carbon quota. Then, substituting into (Equation 6) from (Equation 7), and using an empirical relationship between cellular carbon quota and volume,[27,52,53] $Q_{C,i} = \alpha V_i^{\beta}$, the relationship between N-limited growth rate of the haptophyte-UCYN-A pair and their relative cell sizes can be expressed as

$$\mu_N^{max} = N_N^{max} \frac{1}{\left(\frac{R_H}{R_D}\right)^{3\beta} + 1} \quad \text{(Equation 8)}$$

This relationship is depicted by the red line in Figure 2B. The N-limited case favors a small haptophyte-UCYN-A size ratio because UCYN-A has to supply the nitrogen for both cells. For spherical cells, doubling of host cell radius increases its volume by a factor of 8, along with the required $N_2$ fixation rate; hence the rapid decline with growth rate as the radius ratio increases. The relationship and its intersection with the blue, carbon-limited growth curve, are quite robust to the specific parameter values such as the volume-carbon quota scaling (Figure S2F).

The model reveals the tension between C and $N_2$ fixation which are respectively maximized by a large and small haptophyte–UCYN-A size ratio. Assuming that high growth rate is synonymous with maximizing fitness, the size-ratio at which the carbon- and nitrogen-limited growth rates are equal ($\mu_C^{max} = \mu_N^{max}$) is optimal; indicated by the crossing of blue and red lines in Figure 2B. Algebraically, from (Equation 5) and (Equation 8) we find the optimal ratio

$$\left(\frac{R_H}{R_D}\right)_{opt} = \left(\frac{N_N^{max} E}{P_C^{max}}\right)^{\frac{1}{3\beta}} \quad \text{(Equation 9)}$$

### *Estimating the potential impact of mixotrophy*

Model equation (Equation 5) can be extended to consider the impact of a supplemental carbon-specific, net heterotrophic carbon uptake, $\mu_C^{het}$, (i.e., mixotrophic behavior) as follows:

$$\mu_C^{max} = \frac{P_C^{max}}{E} \frac{\left(\frac{R_H}{R_D}\right)^{3\beta}}{\left(\frac{R_H}{R_D}\right)^{3\beta} + 1} + \mu_C^{het} \quad \text{(Equation 10)}$$

Similarly, the impact of supplemental heterotrophic nitrogen assimilation can be accounted for by the addition of nitrogen-specific, net heterotrophic nitrogen uptake, $\mu_N^{het}$, to (Equation 8):

$$\mu_N^{max} = N_N^{max} \frac{1}{\left(\frac{R_H}{R_D}\right)^{3\beta} + 1} + \mu_N^{het} \quad \text{(Equation 11)}$$

The heterotrophic carbon and nitrogen assimilation rates ($\mu_C^{het}$, $\mu_N^{het}$) may be connected through the stoichiometry of the source. Using Equation 10 and Equation 11 we explored the sensitivity of the optimum size ratio to heterotrophic C and N specific-assimilation rates varying between 0.05 and 0.3 $day^{-1}$, illustrated in Figure S2E.

## Maximum photosynthetic rate

We informed the maximum photosynthetic rate from two data sets, both of which lead to the similar results (Figures S2A and S2B):

### *Taniguchi data compilation*

Data compiled by Taniguchi et al.[21] provide the empirical values for maximum growth rate $\mu_{max}$ for various phytoplankton (Figure S3A). By using only data from haptophytes($\mu_{max}$ = 1.01 (+/−0.25) $d^{-1}$, we estimated $P_C^{max}$ based on $P_C^{max} = \mu_{max}(1+\varepsilon)$ = 1.35 (+/−0.34) $d^{-1}$, since under a steady system, photosynthesis must be balanced by growth (or biosynthesis) and respiration. $\varepsilon$ = 0.341 is a dimensionless coefficient representing the cost of synthesizing average cellular biomass from inorganic substrates and evaluated using basic thermodynamic principles.[28] Note that the sensitivity of $(R_H/R_D)_{opt}$ to the value of $\varepsilon$ is small since (Equation 9) has $E$ in the numerator, which also contains $\varepsilon$.

### *Marañón data*

In a set of consistent laboratory cultures spanning several taxonomic groups and several orders of magnitude in cell volume, Marañón et al.[16] found a unimodal structure in carbon-normalized maximum photosynthetic rate ($P_C^{max}$, $h^{-1}$) as a function of cell volume. The highest $P_C^{max}$ occurred at a cell volume of around 100 $\mu m^3$. The cell volume of the haptophyte host for UCYN-A ranges between of ~4–1500 $\mu m^3$, which is close to the maximum of the $P_C^{max}$ to cell-volume relationship. Within that size range there is no clear trend in the data of Marañón et al[16] (Figure S3B), though individual values vary by a factor of about three. Consistently, the maximum growth

rates of haptophytes ranging between ~20-160 $\mu m^3$ showed no trend with cell volume[21] (Figure S3A). Hence our model assumes a constant $P_C^{max}$ over the relevant range of host sizes. The solid blue line in Figure S2B indicates the solution using the mean $P_C^{max}$ over the range depicted in Figure S3B while the blue shaded region in Figure S2B indicates the range of solutions bounded by the one standard deviation values for $P_C^{max}$ relative to that mean. In the size range of the haptophyte hosts, the mean value is $P_C^{max}$ = 0.126 (+/−0.042) $h^{-1}$ (equivalent to 1.51(+/-0.50) $d^{-1}$ in a 12:12 light:dark cycle).

In Figure 2B we show the result based on Taniguchi data compilation, but the estimate based on Marañón data results in $(R_H/R_D)_{opt}$ values (Figure S2B) are indistinguishable within the margin of uncertainty: $(R_H/R_D)_{opt}$ = 2.47 (+0.27/−0.18) with Taniguchi data compilation, and $(R_H/R_D)_{opt}$ = 2.35 (+0.40/−0.20) with Marañón data.

### Measured specific $N_2$ fixation rates

To evaluate the maximum N-specific $N_2$ fixation rate in the *B. bigelowii*/UCYN-A symbiosis, we used data from Mills et al,[18] which uses $^{15}N$ incubation to track the rate of $N_2$ fixation. We obtained $N_2$ fixation rate per N in UCYN-A in the symbiosis by dividing $N_2$ fixation rate per cell by cellular N in UCYN-A as evaluated by Mills et al.[18] For context, we plotted this with N-specific $N_2$ fixation rates from other $N_2$ fixing cyanobacteria (Figure S3C). We used the highest values, to constrain the *maximum* specific rate. The maximum rates reach more than 10 $d^{-1}$ in UCYN-A and other $N_2$ fixing cells, reflecting the capacity to support not only their own nitrogen demand but also that of partner cells at moderate growth rates (i.e., order of 1 $d^{-1}$). For *Trichodesmium*, *Crocosphaera* and *Nostoc*, we used the data compiled in Inomura et al.[54] To convert from per mol C to per mol N, we have used C:N of 6.3 for *Trichodesmium* and *Nostoc*,[55] and 7.06 for *Crocosphaera* (average based on Großkopf and Laroche[56] and Dron et al.[57]). Since *Nostoc* conducts $N_2$ fixation only in a specific type of cells (heterocysts), we estimated the ratio of N in the trichome to N in the heterocyst based on the volume relationship of the similar organisms, *Richelia*,[58] the volume to C relationship[27] and C:N of 6.3,[55] assuming 1 heterocyst in 15 cells (about an average[59]). We included one value for the $N_2$ fixing soil bacterium, *Azotobacter vinelandii*, estimated from the maximum growth rate,[60] assuming all the fixed $N_2$ is consumed for their growth. Similarly, we estimated a value for $N_2$ fixation rate per cellular nitrogen of heterocysts in Diatom Diazotroph Associations based on the observed growth rate (maximum of 0.87 $d^{-1}$)[58,61,62] and the ratio of the cellular N quota in the symbiosis and the heterocyst ($Q_{N,D}/Q_{N,Het}$), assuming all the fixed N is used for growth.[54] $Q_{N,D}/Q_{N,Het}$ was estimated using, using typical cell count ratios,[54] the relationship between cellular N and cellular volume for multiple phytoplankton[27] and averaged volumes from observations.[58]

## QUANTIFICATION AND STATISTICAL ANALYSIS

Measurements from a total of 167 haptophyte/UCYN-A symbiotic partnerships (Table S1) were used to perform a linear regression analysis ('lm' function in R; package 'stats' version 3.6.2) to investigate whether there is a statistically significant relationship between the volume ($\mu m^3$), in logarithmic scale ($\log_{10}$), of haptophyte cells and their symbiotic UCYN-A (Figure 1B). Similarly, measurements from a total of 108 haptophyte/UCYN-A symbiotic pairs (those with visible chloroplasts) (Table S1) were used to perform a linear regression analysis ('lm' function in R; package 'stats' version 3.6.2) between the volume ($\mu m^3$), in logarithmic scale ($\log_{10}$), of haptophyte cells and their chloroplasts (Figure 1B), and also between the volume ($\mu m^3$) of chloroplasts and UCYN-A within each haptophyte cell (inset Figure 1B). Statistical significance of the volumetric relationships was determined by Student's *t*-test (significance code: ns, non-significant; * at $p < 0.05$; ** at $p < 0.01$; *** at $p < 0.001$; and **** at $p < 0.0001$).

# Supplemental figures

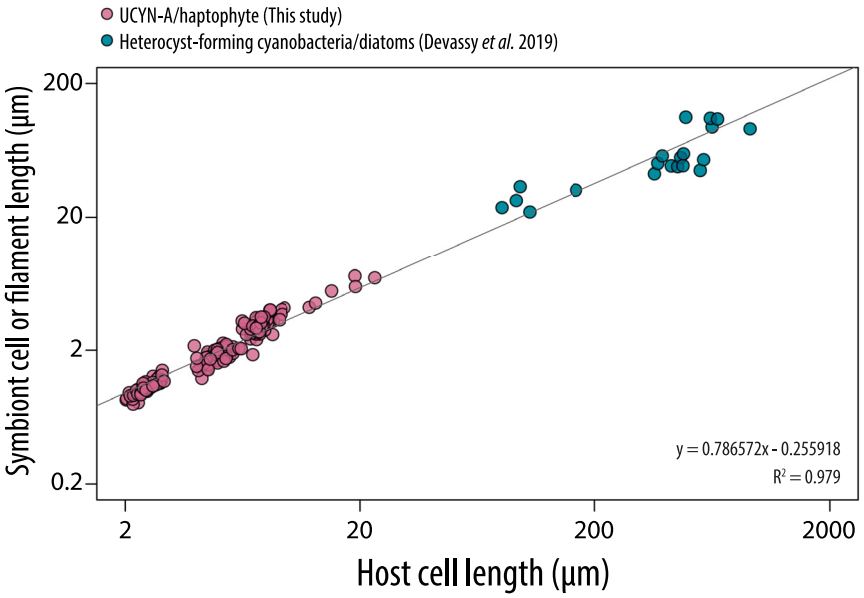


**Figure S1. Cell length relationship between different $N_2$-fixing cyanobacterial/algal symbioses, related to Figure 1B**

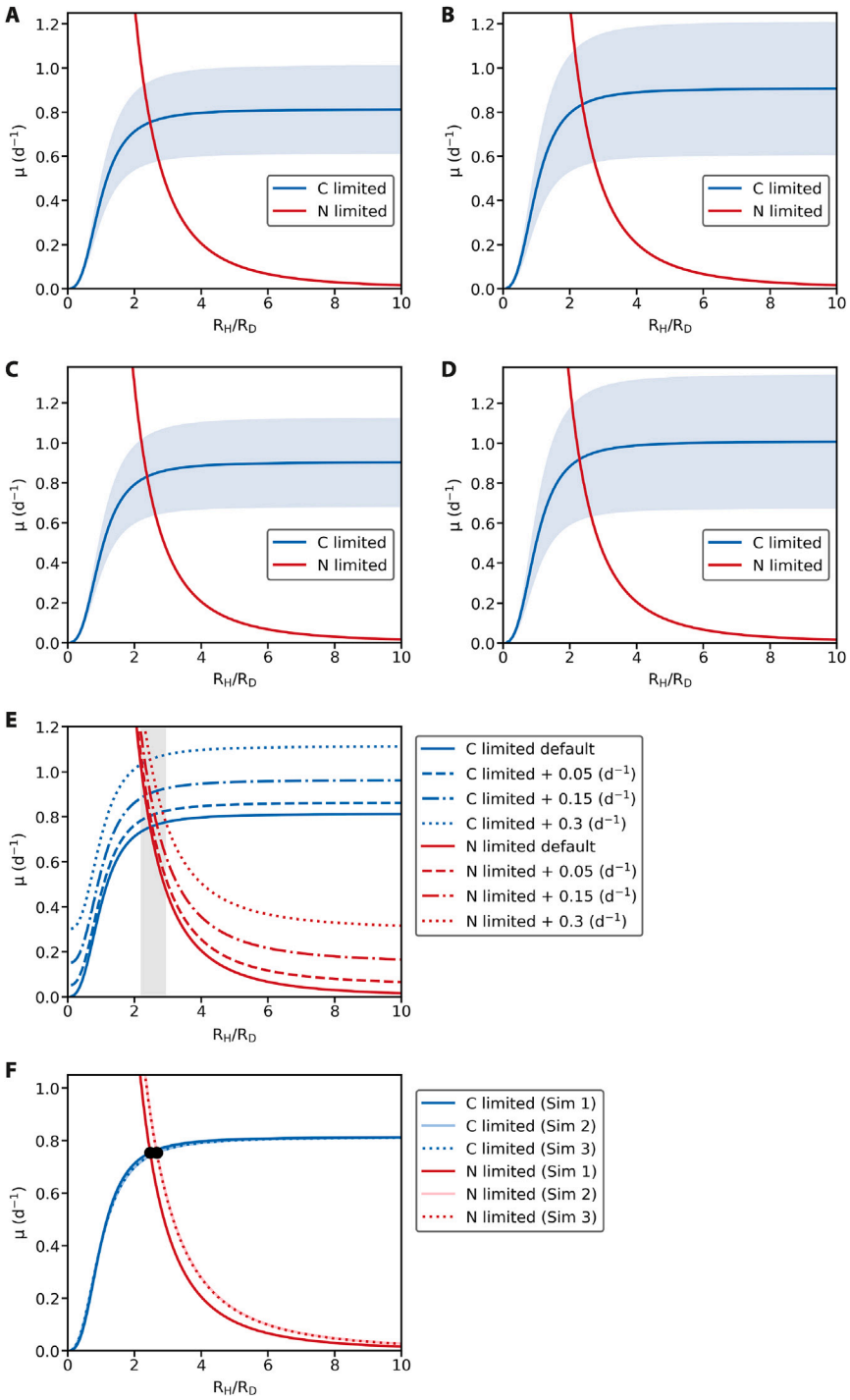


**Figure S2. Predicted growth rate of symbiosis, $\mu$ ($d^{-1}$), vs. ratio of the effective spherical radii of the haptophyte and UCYN-A, $R_H/R_D$, related to Figure 2 and STAR Methods**

(A and B) Model results with $P_C^{max}$ based on Taniguchi data compilation[21] (A) and Marañón data[16] (B), respectively. For the blue curve and shading: the blue curve indicates the predicted relationship when photosynthesis by the host is limiting, and blue shading indicates the range inferred by 1 standard deviation in the C-specific photosynthesis rate in this size range. The red line is the modeled maximum growth rate when $N_2$ fixation by UCYN-A is limiting, calibrated by the maximum observed N-specific $N_2$ fixation rate in UCYN-A.[18] The highest growth rate occurs at the radius ratio where the blue and red lines cross $(R_H/R_D)_{opt}$ and the inferred $(R_H/R_D)_{opt}$ values are consistent: 2.47 (+0.27/−0.18) for (A) and 2.35 (+0.40/−0.20) for (B).

(C and D) Model simulations with potential light harvesting by UCYN-A. In these simulations, the energetic cost of $N_2$ fixation[63] is set to zero, based on the assumption that the cost is covered by light harvesting by UCYN-A. (C) and (D) are the results of the model simulation with $P_C^{max}$ based on Taniguchi data

*(legend continued on next page)*

compilation[21] (C) and Marañón data[16] (D), respectively. $(R_H/R_D)_{opt}$ values are similar to those in (A) and (B): 2.38 (+0.26/−0.18) for (C) and 2.25 (+0.40/−0.20) for (D).

(E) Model's sensitivity to heterotrophic carbon and nitrogen uptake of the haptophyte. The solid lines are the same as in Figure 2B. The additional dashed lines indicate the effects of a supplemental acquisition of carbon (blue dashed) and nitrogen (red dashed), with net specific uptake rates varying between 0.05 and 0.3 $day^{-1}$), independent of carbon and $N_2$ fixation. (See Equations 10 and 11 in STAR Methods.) We note that the crossing of the blue and red lines (the optimal cell size ratio) is relatively insensitive to the degree of heterotrophic nutrition, as highlighted by the gray shading.

(F) Model's sensitivity to the imposed relationship between cell volume and carbon quota. Here, we used three published estimates for power-law relationships from Menden-Deuer and Lessard,[27] Verity et al.,[52] and Strathmann[53]: Sim1–3, respectively. Each simulation (Sim1–3) finds a slightly sub-linear power-law relationship leading to very similar predictions for $(R_H/R_D)_{opt}$ (black circles: crossing of red and blue curves).

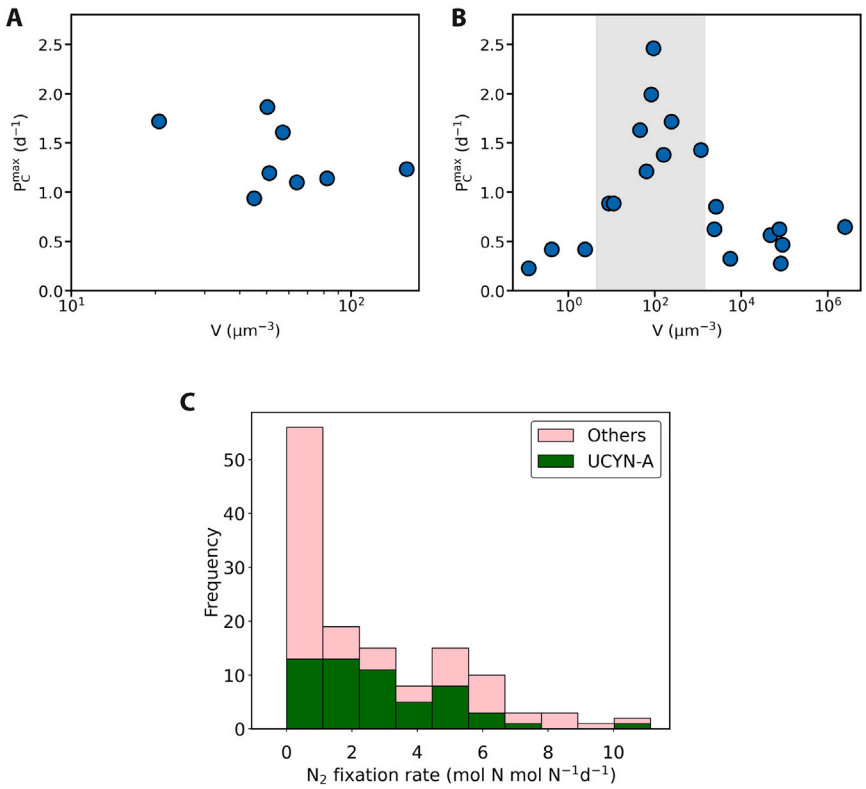


**Figure S3. Specific carbon and nitrogen fixation rates, related to STAR Methods**

(A and B) Specific carbon fixation rates ($P_C^{max}$) shown as a function of cell volume.

(A) $P_C^{max}$ inferred from $\mu_{max}$ data for haptophytes from Taniguchi et al.[21]

(B) $P_C^{max}$ as a function of cell size from the laboratory cultures of Marañón et al.[16] Units converted from $h^{-1}$ based on 12:12 light-dark cycle as in the experiment.[16] The gray shading shows the volume range of haptophyte relevant to the hosts in this study.

(C) Histogram of the (per N-fixing cell or spheroid body) N-specific $N_2$ fixation rate from UCYN-A and other $N_2$-fixing cyanobacteria. The y axis represents the frequency of measured N-specific $N_2$ fixation rates compiled from published studies detailed in "Measured specific $N_2$ fixation rates" in method details.